EVALUATION OF INHIBITORY ACTIVITY CHITOSAN NANOPARTICLES LOADED ON BASIL OIL AGAINST *PSEUDOMONAS AERUGINOSA* BIOFILM FORMATION

Ahmed Abdul Kadhim Obeid* **Emad Hamdi Jassim**
Lecturer **Assist. Prof.**
Genetic Engineering and Biotechnology Institute, University of Baghdad.
ahmed.obaid2100m@ige.uobaghdad.edu.iq

ABSTRACT

The increasing resistance of *Pseudomonas aeruginosa* to antibiotics has complicated the treatment of infections due to its various virulence factors. One of its major pathogenic traits is the ability to form thick biofilms, which allow the bacteria to adhere to living or nonliving surfaces and enhance drug resistance. Consequently, exploring safe and effective therapeutic alternatives from plant sources has become essential for combating this multidrug-resistant pathogen. In this study, essential oil of *Ocimum basilicum* (BEO) was extracted via distillation and analyzed by GC-MS. The BEO was then loaded onto chitosan nanoparticles (BEOCSNPs) prepared using the ionic gelation method with tripolyphosphate (TPP). The nanoparticles were characterized using UV–vis, FTIR, SEM, and XRD techniques. Clinical isolates of *Pseudomonas aeruginosa* were obtained and identified with the VITEK-2 system. The minimum inhibitory concentrations (MICs) of BEO and BEOCSNPs were determined using a 96-well resazurin-based microdilution assay. The MIC of BEO ranged from 190 to 95 µg/mL, whereas the MIC of BEOCSNPs was significantly lower, ranging from 3.75 to 0.93 µg/mL. The inhibitory effects at sub-MIC concentrations were assessed by measuring optical density in a 96-well microplate using 0.1% crystal violet staining, which showed a significant decrease in biofilm formation. The biofilm inhibition activity of BEOCSNPs was notably higher in isolates P16 and P22, with inhibition percentages of 84.28% and 79.32%, respectively. In comparison, BEO alone inhibited P16 and P22 at 66.74% and 57.43%, respectively. These results indicate that *Ocimum basilicum* essential oil loaded onto chitosan nanoparticles exhibits superior inhibitory activity against biofilm formation of *Pseudomonas aeruginosa* compared to the essential oil alone.

Keywords: antibacterial , GC-MS , pathogenic bacteria, MDR.

تقييم النشاط التثبيطي لدقائق الكيتوسان النانوية المحملة على زيت الريحان ضد تكوين الأغشية الحيوية لـ *Pseudomonas aeruginosa*

احمدعبد الكاظم عبيد عماد حمدي جاسم
باحث استاذ مساعد
معهد الهندسة الوراثية والتقنيات الاحيائية. جامعة بغداد.العراق

المستخلص

أدى تزايد مقاومة *Pseudomonas aeruginosa* للمضادات الحيوية إلى صعوبة علاج العدوى بسبب عوامل الضراوة المتعددة لهذه البكتيريا. ومن أهم خصائصها الممرضة قدرتها على تكوين أغشية حيوية سميكة (Biofilms) ، مما يسمح للبكتيريا بالالتصاق بالأسطح الحية وغير الحية ويزيد من مقاومتها للأدوية. لذلك، أصبح البحث عن بدائل علاجية آمنة وفعالة من المصادر النباتية ضروريًا لمكافحة هذه البكتيريا المقاومة متعددة الأدوية.في هذه الدراسة، تم استخراج زيت القرنفل العطري من نبات *Ocimum basilicum* (BEO) بواسطة التقطير وتحليله باستخدام GC–MS . بعد ذلك، تم تحميل الزيت على جسيمات نانوية من الكيتوسان (BEOCSNPs)باستخدام طريقة الجل الأيوني (ionic gelation) مع ثلاثي فوسفات الصوديوم.(TPP) وتم توصيف الجسيمات النانوية باستخدام تقنيات UV–vis، FTIR، SEM، و.XRD تم الحصول على عزلات سريرية من *Pseudomonas aeruginosa* وتحديدها باستخدام نظام .VITEK–2تم تحديد التركيز المثبط الأدنى (MIC) للزيت العطري وجسيمات BEOCSNPs باستخدام طريقة الميكروتيوتر 96- well لقائمة على الريزازورين .تراوحت قيمة MIC للزيت العطري بين 190و95 µg/Ml ، بينما كانت MIC لجسيمات BEOCSNPs أقل بكثير، بين 3.75و .0.93 µg/mL وتم تقييم التأثيرات المثبطة عند تركيزات أقل من MIC بقياس الكثافة الضوئية (OD) في ألواح ميكروتيتر 96 باستخدام صبغة الكريستال البنفسجية 0.1%، وأظهرت النتائج انخفاضًا ملحوظًا في تكوين الأغشية الحيوية . كان نشاط مثبط الأغشية الحيوية لجسيمات BEOCSNPs أعلى بشكل واضح في العزلات P16وP22، حيث بلغت نسب التثبيط 84.28%و 79.32%على التوالي. بالمقارنة، كان تثبيط الزيت العطري وحده للعزلات P16 و 66.74% P22و 57.43%على التوالي. تشير هذه النتائج إلى أن زيت *Ocimum basilicum* المحمل على جسيمات الكيتوسان النانوية يمتلك نشاطًا مثبطًا أكبر لتكوين الأغشية الحيوية لـ *Pseudomonas aeruginosa* مقارنة بالزيت العطري وحده.

الكلمات المفتاحية: مضاد بكتيري، كروماتوغرافيا الغاز– مطياف الكتلة ، البكتريا المسببة للامراض ،المقاومة المتعددة للادوية.

Received:2 /5/2023, Accepted:22/10/2023, Published:December 2025

INTRODUCTION

Multidrug-resistant bacteria have become a problem in recent years as a result of incorrect or excessive use of antibiotics. Several microorganisms, including bacteria, fungi, viruses, and parasites, are responsible for antibiotic resistance. As a result, the problem is increasingly recognized as a growing global hazard. As a result, novel and creative antimicrobial alternatives are desperately required to solve the multidrug resistance issue (1). The use of medicinal plants in therapeutics and prophylaxis is promising and is, despite what has been accomplished at this time. Research to select effective chemicals from medicinal plant extracts is still ongoing (10). Basil (*Ocimum basilicum L*.) is becoming more well-known due to the powerful ingredients present in the essential oils of its leaves and branches. *Pseudomonas aeruginosa* bacteria were thought to be the most harmful bacterial species because they are resistant to the majority of medications, producing a wide range of ailments, one of the most virulent factors of this bacteria is the formation of biofilm (14). The biofilm is linked to high resistance to external stress, resistance to antibiotics (2), and host defenses for which disinfectant therapy is ineffective. Virulence factors are molecules synthesized by pathogenic microorganisms that enhance their capacity to evade host immune defenses and establish infection (23). Chitosan is recognized as the second most abundant naturally occurring biopolymer after cellulose. It is a biodegradable and biocompatible substance derived primarily from the exoskeletons of crustaceans and other arthropods (19). The design, manufacture, and manipulation of particles with structures spanning from 1 to 100 nanometers is an important field of current research. Nanoparticles made of chitosan are cationic, biodegradable, almost non-toxic, and biocompatible. Therefore, they are widely used in biological applications such as drug delivery (26). This study aimed to develop a novel, safe, and effective formulation by incorporating basil essential oil extract into chitosan nanoparticles and to evaluate its inhibitory activity against biofilm formation by Pseudomonas aeruginosa.

MATERIALS AND METHODS

Essential oil extraction : Distillation is used to separate essential oils. According to the literature, dried basil was first weighed (100 g), placed in a distillation apparatus (0.5 L distilled water), and steam distilled for 4 hours using a Clevenger apparatus. The essential oil was then evaporated with the steam and collected in a condenser. Anhydrous sodium sulfate was used to separate the still-mixed oil and water. Extracted essential oils are placed in dark-sealed bottles and kept refrigerated (17).

Identification of components by (GC-MS): The chemical composition of basil essential oil (BEO) was analyzed using an Agilent 7820A GC–MS system. A 1 µL sample was injected, with the oven temperature set at 70 °C and the injector maintained at 250 °C, for a total run time of approximately 34 minutes. The constituents of BEO were identified by comparing the obtained chromatographic peaks and retention times with reference spectra from the Wiley mass spectral library (3).

Chitosan nanoparticle biosynthesis: The basil essential oil (BEO) was encapsulated into chitosan nanoparticl es through a two-step procedure involving ionic gelation followed by oil-in-water emulsification. A 5% chitosan solution was prepared by dissolving 200 mg of chitosan in 100 mL of acetic acid, after which 12 mL (7%) of basil oil was added to the solution. Tripolyphosphate (TPP) was then introduced to the chitosan–BEO mixture following the ionic gelation technique to form chitosan nanoparticles loaded with BEO (CSNPs–BEO). The TPP solution was added to the chitosan–BEO mixture at a 1:2.5 (w/w) ratio and continuously stirred at room temperature for six hours. The formation of nanoparticles was achieved through ionic crosslinking of chitosan initiated by TPP. The resulting CSNPs–BEO were subsequently separated, thoroughly washed, and centrifuged to remove the supernatant. The obtained precipitate was then resuspended in distilled water and dried for further analysis (27).

Characterization (morphological and structural) of CSNPs loaded BEO: Many various approaches were used to characterize

(morphological and structural) to identify CSNPs loaded BEO in this study.

Utilizing the HPLC method to measure the chemical concentration in BEO and BEO loaded with CSNPs : One of the most newest and successful techniques for identifying the predominant chemical group in basil essential oil was described as using reversed-phase HPLC analysis of Essential Oil of *Ocimum basilicum* and CSNPs loaded BEO. High-performance liquid chromatography (HPLC) was conducted using a SYKAMN HPLC system (Germany) fitted with a C18-ODS column (250 × 4.6 mm, 5 µm). A 100 µL sample was injected, and separation was achieved using a mobile phase composed of solvent A (95% acetonitrile with 0.01% trifluoroacetic acid) and solvent B (5% acetonitrile with 0.01% trifluoroacetic acid) at a flow rate of 1 mL/min. Detection of the compounds was performed with a UV–visible detector set at 280 nm, while quantification of eugenol was determined from calibration curves and peak area analysis (11). The concentrations are calculated according to equation (1):

$$\textbf{Sample concentration} = \frac{\textit{Concentration std.} * \textit{Area sample}}{\textit{Area std.}} * \textbf{DF} \quad \ldots. \quad (1)$$

DF: Dilution factor

Samples Collection: Several clinical samples were collected (swabs) were collected from patients hospitalized in Baghdad who suffered from burn infections and under the supervision of a specialist. Samples were taken using sterile swabs with a transport medium, and they were immediately cultured on blood agar media, MacConkey agar media, and Cetrimide agar (for isolation and initial diagnosis of bacteria) and kept at 37°C for 24 hours to allow for further, confirmatory testing.

Estimation of the MIC and Sub-MIC: The antibacterial efficacy of *Ocimum basilicum* essential oil and its chitosan nanoparticle (CSNP)-loaded formulation was assessed against the Gram-negative bacterium *Pseudomonas aeruginosa* using minimum inhibitory concentration (MIC) and sub-minimum inhibitory concentration (Sub-MIC) assays. The MIC values were determined through the resazurin-based microdilution method in Mueller–Hinton broth (MHB), employing a 96-well microtiter plate (9).

Test substance's impact on biofilm development: The microtiter plate (MTP) assay is a qualitative method used to evaluate the ability of tested agents to inhibit biofilm formation, with measurements obtained using a microplate reader. Sub-MIC concentrations, determined in prior experiments, were used to evaluate the inhibitory effects of the tested materials on biofilm development, and biofilm quantification was performed following the method described by (12). The optical density (OD) of each well was determined at a wavelength of 600 nm using an ELISA microplate reader. The absorbance values of the blank wells served as negative controls for determining biofilm formation by the isolates. Isolates exhibiting OD values higher than those of the blank wells were considered biofilm producers. The cutoff optical density (ODc) value was used to classify bacterial isolates according to their ability to form biofilms. The ODc was calculated using the following equation:

ODc = Average OD of the negative control + (3 × standard deviation (SD) of the negative control) … (2)

The OD value for each isolate was then determined as:

OD isolate = Average OD of the isolate – ODc … (3)

Based on the obtained OD values, bacterial adherence was categorized as follows:

OD ≤ ODc: Non-adherent

ODc < OD ≤ 2ODc: Weak adherence

2ODc < OD ≤ 4ODc: Moderate adherence

OD > 4ODc: Strong adherence

The plates were incubated at 37 °C, after which the wells were gently rinsed and stained. Absorbance was measured at 600 nm using a microplate reader, and the percentage of biofilm inhibition was calculated according to Equation (4 ((21).

% Biofilm inhibition = [(OD Control- OD Sample)/OD Control] ×100……(4). The experiment is conducted with three replicates of the test material

Statistical analysis: The Statistical Analysis System (SAS) software (31) was used to evaluate the effects of various factors on the study parameters. Significant differences between means were assessed using analysis

of variance (ANOVA), followed by the least significant difference (LSD) test.

RESULTS AND DISCUSSION

Isolation of essential oil of *Ocimum basilicum:* The effectiveness of this approach may be evaluated by the extraction yield. The yield of the oil of *Ocimum basilicum* extract in the current investigation was 0.67± 0.05%. The findings of the present study support the researcher's assertions (24). Plant genotypes and other factors have the most impact on the composition of oils in medicinal and aromatic plants.

GC-MS Analysis: The retention times, percentage composition, and chemical structures of *Ocimum basilicum* components, as determined by gas chromatography–mass spectrometry (GC–MS), are presented in Table **).**(Fig. 1) shows a typical GC MS histogram with 20 significant peaks showing that 20 volatile chemicals in basil essential oil are the same as the reference molecules, The components, which make up 99.986% of the discovered basil oil, come from three separate hydrocarbon groups: sesquiterpenes, oxygenated monoterpenes, and phenylpropene. . According to the results, basil leaves had 45.24 % more linalool than the average ingredient in this sample.

Table1. Chemical Composition of essential oils. *Ocimum basilicum*

No. Peak	RI	Compounds	Chemical Formula	Area (%)
1	9.926	β-element	C15H24	0.225%
2	11.453	α-bergamotene	$C_{15}H_{24}$	1.316
3	16.758	Farnesene	C15H24	0.344%
4	23.167	Borneol	C10H16O	11.21
5	23.723	α-copaene	C15H24	1.006%
6	25.375	1,8-Cineole	C10H18O	16.64
7	25.471	Linalool	C10H18O	45.24
8	25.545	β-caryophyllene	C15H24	2.146
9	25.777	Eugenol	C10H12O2	2.768
10	25.997	Geraniol	C10H18O	4.61
11	26.270	Neral	C10H16O	7.24
12	26.537	Chicoric acid	C22H18O12	1.270
13	27.001	Estragole	C10H12O	2.077
14	29.116	Methyl eugenol	C11H14O2	0.417
15	29.617	Germacrene	C15H24	0.359
16	30.173	Guaiene	C15H24	0.686
17	31.333	Azulen	C10H8	0.95
18	31.553	Guaiazulene	C15H18	0.446
19	32.557	α –Himachalene	C15H24	0.569
20	34.980	α –Bisabolene	C15H24	0.467
Total				99.986

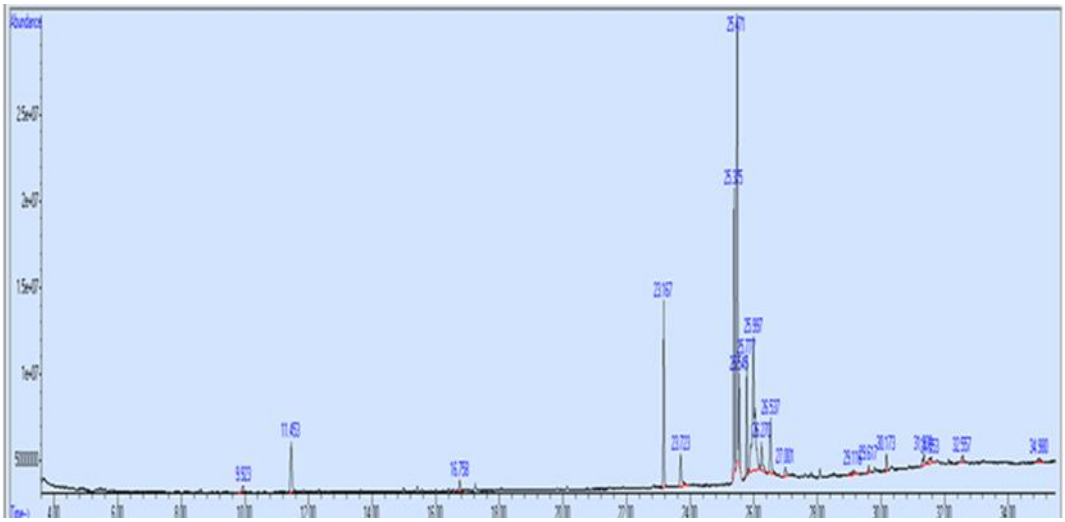

Figure 1. Typical GC-histogram of essential oils. *Ocimum basilicum*

Chitosan nanoparticle biosynthesis

positively charged chitosan (CS) and negatively charged tripolyphosphate (TPP) at room temperature. During this process, TPP electrostatically interacts with the NH_3^+ groups of CS, leading to the formation of ionically cross-linked CS nanoparticles (CSNs) (4) .more researchers (15). It has been reported that incorporating essential oils into chitosan is among the most effective strategies for drug delivery, due to the formation of amide bonds between the carboxyl groups of plant essential oils and the primary amino groups of chitosan, without requiring spacer molecules. In this study, the essential oils were loaded into chitosan, resulting in a cage-like structure formed by the self-association of the hydrophobic segments of basil essential oil within and around the chitosan matrix, while the hydrophilic segments remained exposed. The appearance of a clear color indicates the formation of nanoparticles loaded with the plant extract. hue The fig. is 2.

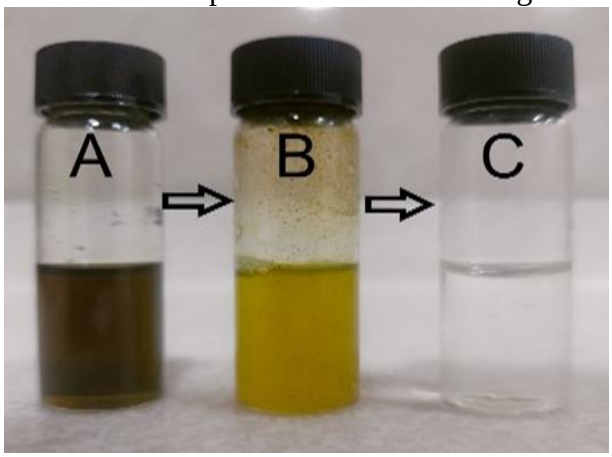

Figure 2. Steps of CSNPs loaded BEO preparation A:BEO, B:BEO/CS, C:CSNPs loaded BEO

Characterization of CSNPs loaded BEO

UV-Visible spectroscopy: With UV-visible spectroscopy, the synthesis of CSNPs-rich BEO is first confirmed. The absorbances of BEO and BEO that had been loaded with CSNPs were tested; the results are shown in Fig.3 and Table 2 for BEO and CSNPs-loaded BEO. (Fig.4) (Table 3). The greatest absorbance value in the BEO was 1.082, The lowest absorbance values for BEO were 0.301 at wavelengths of 240 nm and 291 nm, respectively. For CSNPs loaded with BEO, the highest absorbance was 0.248, while the lowest was 0.196 at 286 nm and 329 nm, respectively. Notably, the absorbance at 669 nm decreased from 0.270 in BEO to 0.065 in CSNPs loaded with BEO. Additionally, the maximum absorbance shifted from 1.082 at 291 nm in BEO to 0.248 at 286 nm in CSNPs loaded with BEO. A new strong absorption peak also appeared at 416 nm with a value of 0.306 in CSNPs loaded with BEO. These findings confirm the successful synthesis of the nanomaterial and the efficient encapsulation of BEO within the chitosan nanoparticles.

Table 2. UV-visible spectral analysis results of BEO

Peak No.	Wavelength /nm	Absorbance
1	669.00	0.270
2	291.00	1.082
3	240.00	0.301

Table 3. UV-visible spectral analysis results of CSNPs loaded BEO

Peak No.	Wavelength /nm	Absorbance
1	673.00	0.130
2	615.00	0.065
3	537.00	0.079
4	484.00	0.175
5	455.00	0.205
6	416.00	0.306
7	329.00	0.196
8	286.00	0.248

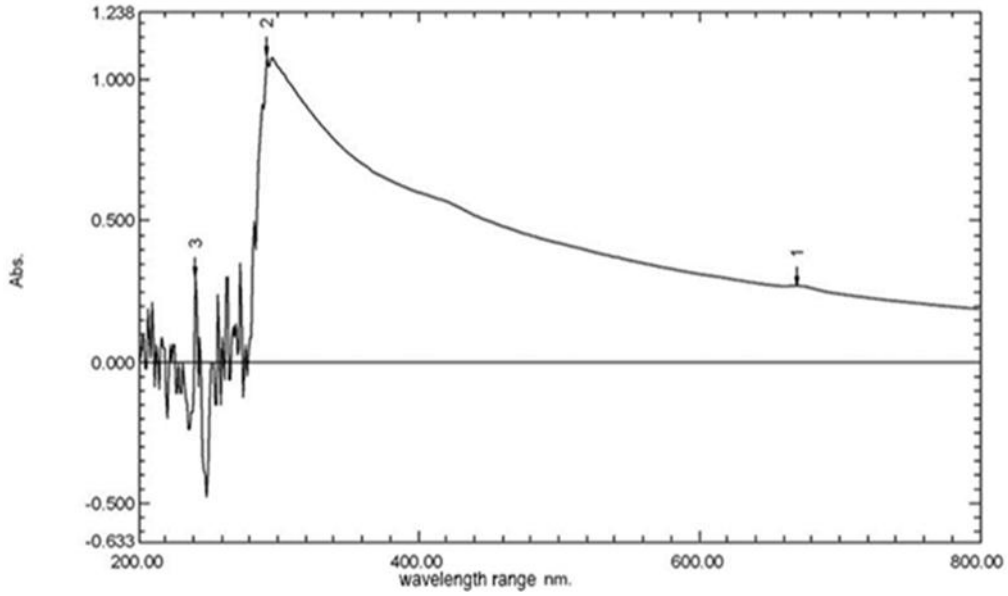

Figure 3. UV-visible spectral analysis of BEO

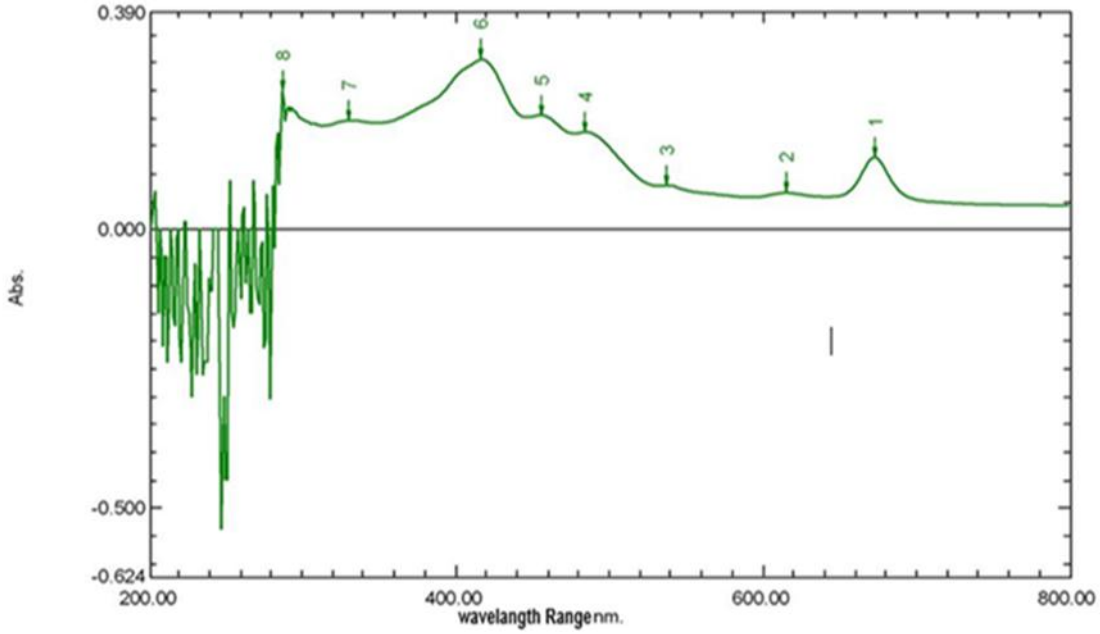

Figure 4. UV-visible spectral analysis of CSNPs loaded BEO

Fourier transformation infrared spectroscopy (FTIR) : In this study, the functional groups of chitosan (CS) were confirmed, and changes in the chemical groups of basil essential oil (BEO) upon loading into chitosan nanoparticles (CSNPs) were observed. (Fig.5) shows the FTIR spectrum of chitosan, where the peak at 3427.51 cm^{-1} corresponds to the symmetric stretching vibration of O–H, and the peak at 2924.09 cm^{-1} indicates C–H stretching. Additional peaks include amide stretching and C=O stretching, observed at 1134.14 cm^{-1} and 1523.76 cm^{-1}, respectively. (Fig.6)presents the FTIR spectrum of CSNPs loaded with BEO, showing multiple peaks: the first at 447.49 cm^{-1}, corresponding to the out-of-plane bending of NH and C=O; 615.29 cm^{-1}, attributed to -CCH vibrations; and 943.19 cm^{-1} and 993.34 cm^{-1}, associated with C–O–C stretching. Peaks at 1149.57 cm^{-1} are related to in-plane O–H bending of aromatic compounds, indicating the presence of terpenoids and flavones in the basil oil extract. The amide III band with C–N stretching appears at 1398.39 cm^{-1}, while the amide I group is observed at 11618.28 cm^{-1}. Peaks at 2090.84 cm^{-1} and 2185.35 cm^{-1} are attributed to CO_2 bending vibrations, and the peak at 2924.09 cm^{-1} is contributed by aromatic components. Comparison of the spectra of CS and CSNPs loaded with BEO revealed new peaks at

447.49, 2090.84, and 2185.35 cm^{-1}, which were absent in pure chitosan. These new peaks indicate the formation of new chemical bonds, suggesting the generation of new compounds upon loading BEO into chitosan nanoparticles.

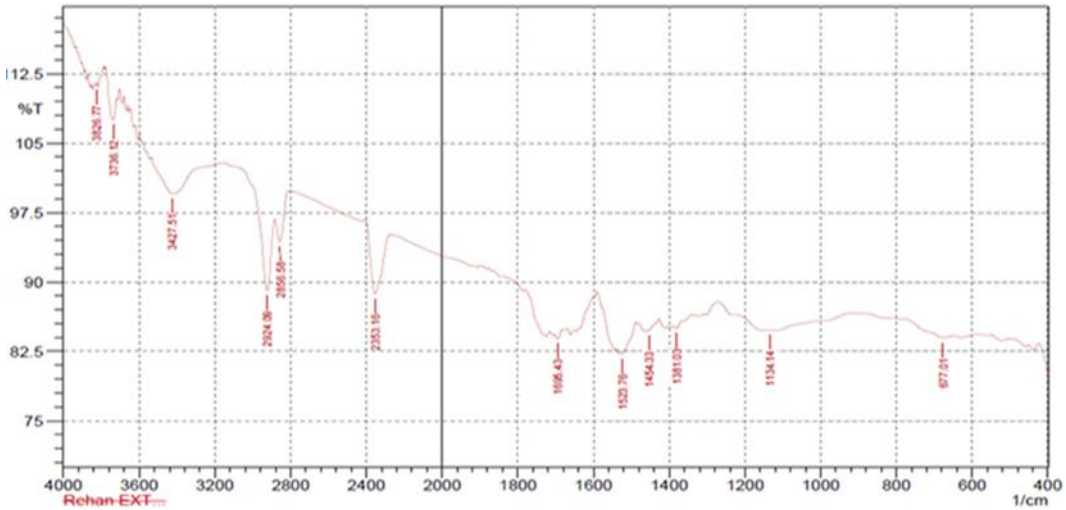

Figure 5. FTIR Spectra Pattern of CS

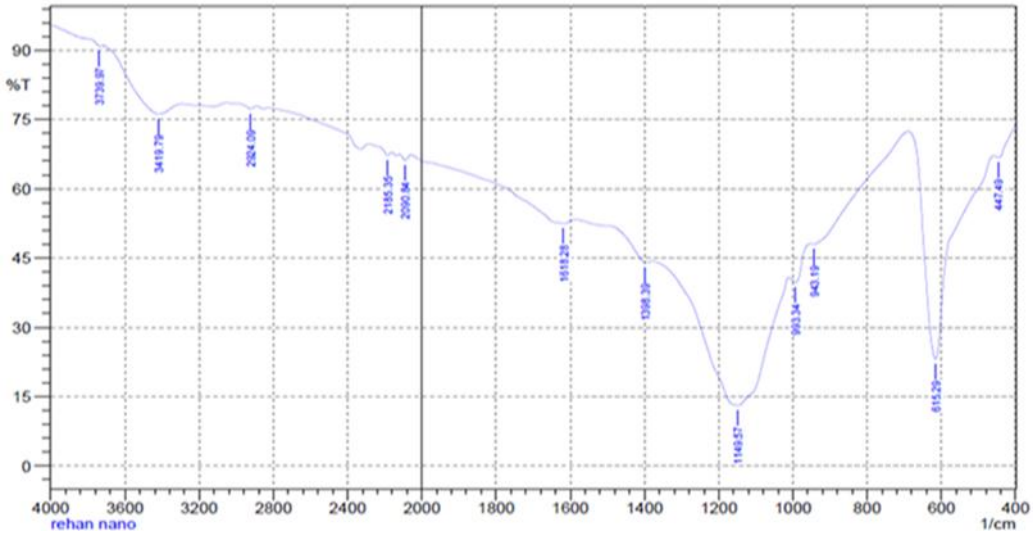

Figure 6. FTIR Spectra Pattern of CSNPs loaded BEO

Diffraction of X-rays (XRD)

A significant peak of 2θ value at 20.53° and an intensity level equivalent to 1200 cont. are seen in the chitosan X-ray diffraction patterns (Fig. 7), on the other hand, depicts the XRD pattern of a BEO sample containing CSNPs. Five distinct peaks at 2θ were at 18.88, 26.67, 31.93, 35.72, and 38.04° (Fig.8) this alteration illustrates how the crystal structures of the two materials differ, with BEO loaded with CSNPs being more crystalline than CS and exhibiting a displacement from the peaks of natural chitosan. In this study, the previously identified 20.53° peak of the CS diffraction has moved to a higher value of 38.04°. This may be related to how CS loaded with BEO interacts to produce CSNPs loaded BEO. According to (29), the apex lies approximately 2θ = 30°. It might be a symptom of the existence of some elements loaded on chitosan, which backs up the study's conclusions concerning the high degree of crystallization of chitosan loaded with basil essential oil.

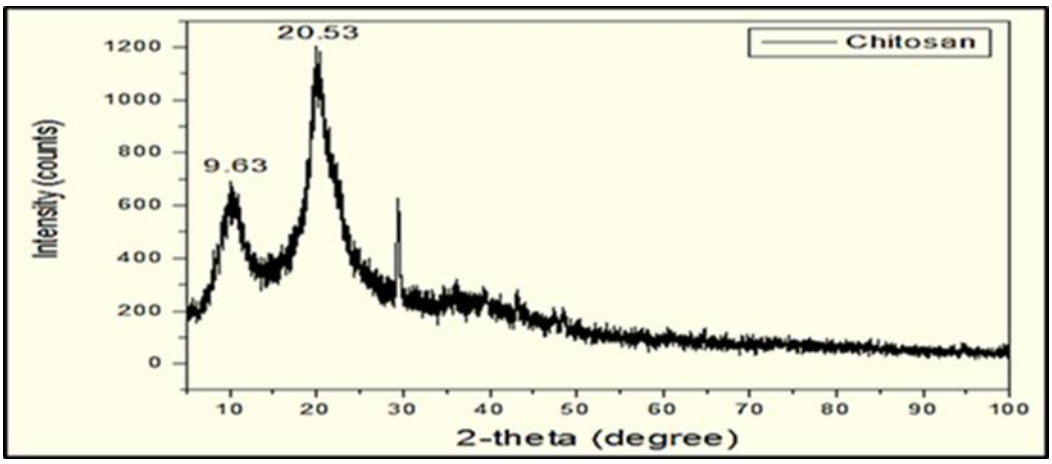

Figure 7. Diffractogram of CS (6)

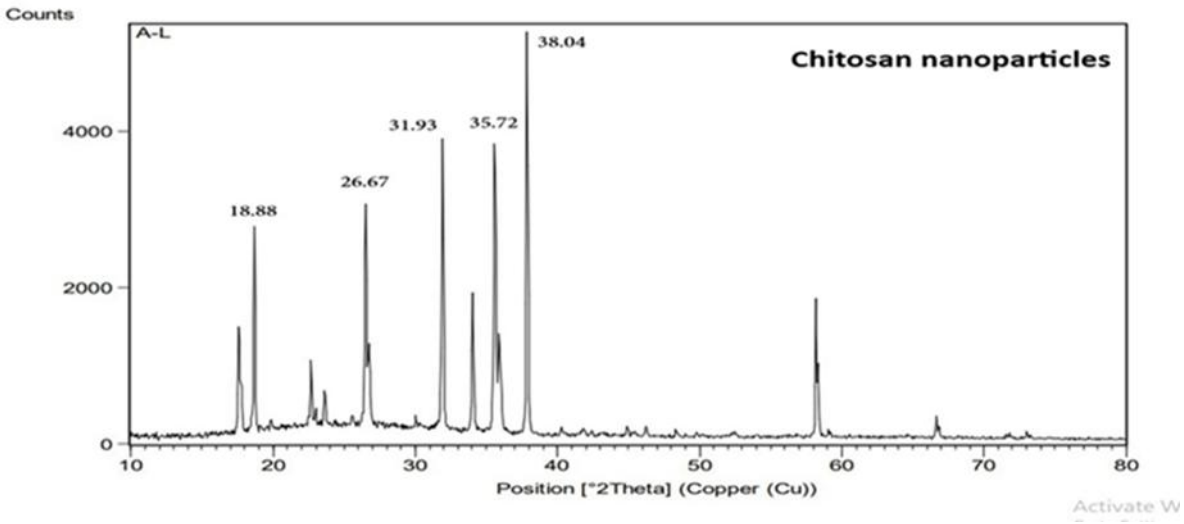

Figure 8. Diffractogram of CSNPs loaded BEO

Scanning Electron Microscope (SEM)

The morphology of CSNPs loaded with BEO was analyzed using scanning electron microscopy (SEM), as illustrated in Figure 4-9. The nanoparticles exhibited a spherical shape with diameters ranging from 50.31 to 64.09 nm and showed a relatively uniform morphology. (20)found that the majority of the biosynthesized CNPs synthesized CNPs have average particle sizes ranging from 33.64 to 74.87 nm. Considering that phytochemicals have a main role in formation of CNPs ,it can be said that whatever be smaller the size of this phytochemicals existing in the plant extract, as aresult will be smaller obtained particle size(18).

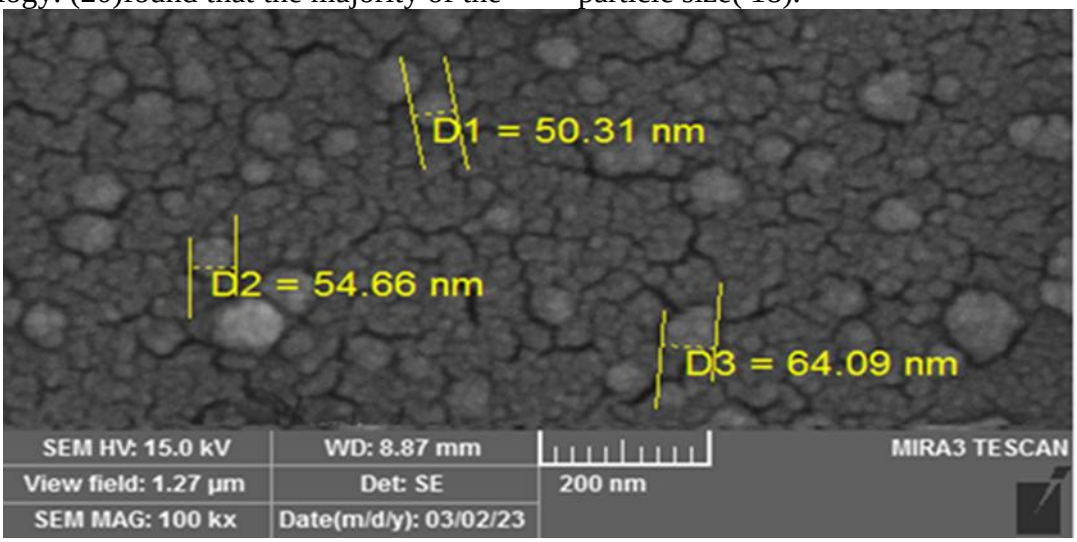

Figure 9. Scanning Electron Microscopy image of CSNPs loaded BEO

Potential zeta: created nanoparticles, because of the higher electrostatic repulsion, CNPs show good stability in thin study when applied to the loaded BEO surface with CSNPs (Fig. 10). According to (25), for an NP suspension to be sustained predominantly by electrostatic repulsion, It is important to have a zeta potential of at least 30 mV. CNPs are less stable if the zeta potential is less than + 30 mV because of lower electrostatic repulsion. CNPs are more powerful because they have a positive zeta potential, which indicates they have a charge.

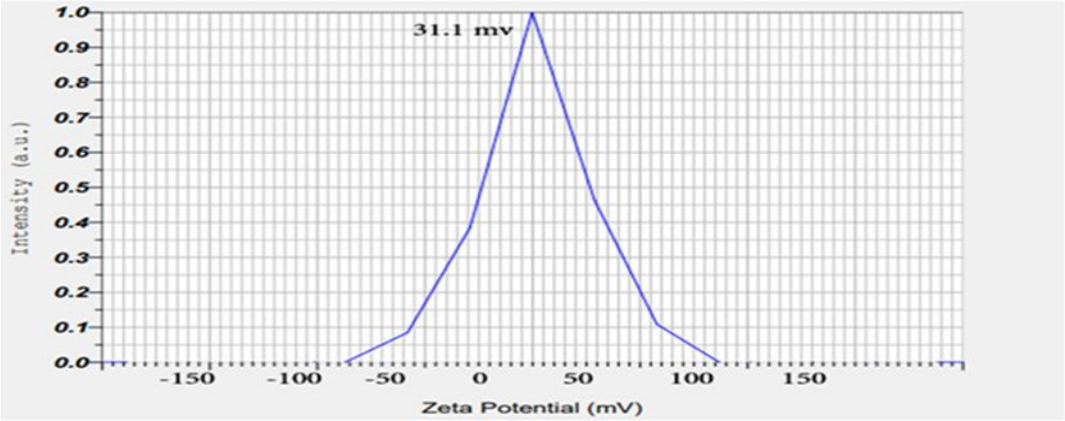

Figure 10. Zeta potential of CSNPs loaded BEO (+31.1) Mv

Determination of the concentration of Chemical compounds in BEO and CSNPs loaded BEO using the HPLC technique: HPLC investigation revealed the existence of 5 chemical components in BEO and CSNPs loaded BEO. All the identified compounds appear to have different retention times. Higher concentrations of Chemical compounds of BEO were Linalool (115.67 µg/ml),1,8-Cineole (99.39 µg/ml), Borneol (66.3 µg/ml), Neral (63.1 µg/ml), and Geraniol (38.19) While the higher concentrations compounds of CSNPs loaded BEO were Linalool (9.25 µg/ml), 1,8-Cineole (6.1 µg/ml), Borneol (5.7), Neral (5.4) ,and Geraniol (4.1). These constituents' concentrations are shown in (Table 4) and (Fig.11 and 12).

Table 4. The calculated concentrations of Chemical compounds BEO and CSNPs loaded BEO from HPLC results.

Chemical compounds (µg/ml)	BEO	CSNPs loaded BEO
Linalool	**115.67**	**9.25**
1,8-Cineole	**99.39**	**6.1**
Borneol	**66.3**	**5.7**
Neral	**63.1**	**5.4**
Geraniol	**38.19**	**4.1**
Total concentration (µg/ml)	**382.65**	**30.55**

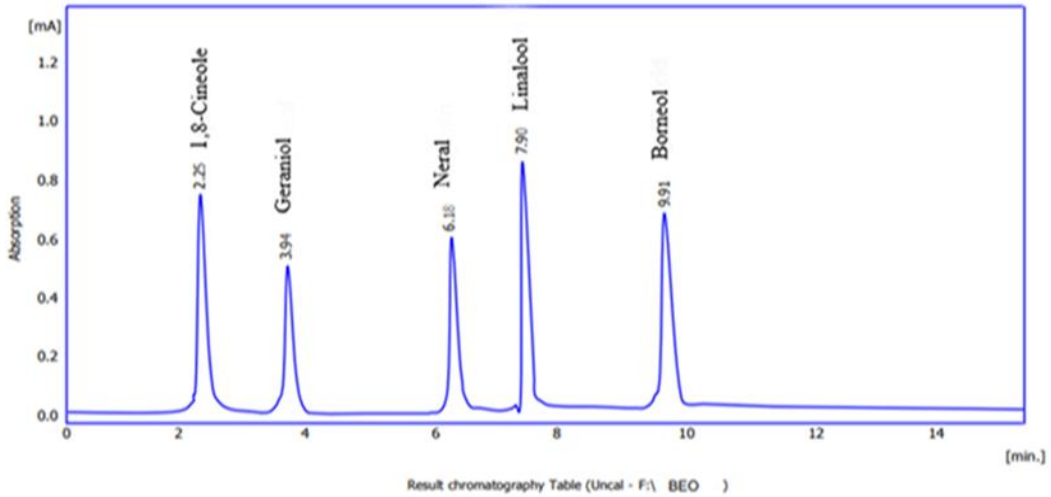

Figure 11. HPLC chromatogram of Chemical compounds in BEO

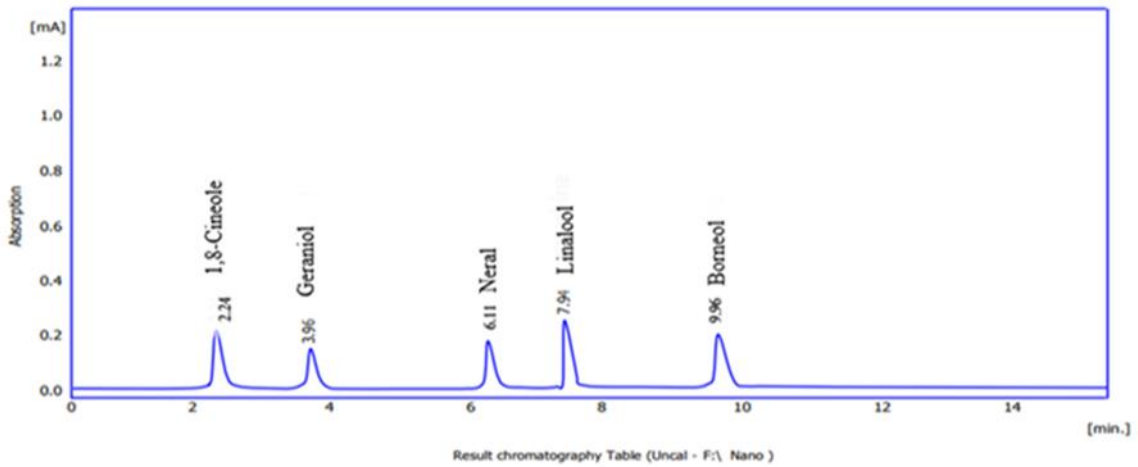

Figure 12. HPLC chromatogram of Chemical compounds in CSNPs loaded BEO

Bacterial Biofilm Formation Detection: In this study, the biofilm-forming ability of 29 out of 40 Pseudomonas aeruginosa isolates was assessed using a microtiter plate (MTP) assay. The optical density (OD) of each well was measured at 600 nm with an ELISA reader. The generated Biofilm was adhered on polystyrene microplates in this study.The biofilm development results were compared to those of other authors (28), who found that the microorganism can form biofilm using the MTP method As a positively charged stain, Crystal Violate attaches to negatively charged components such as polysaccharides, proteins, and nucleic acids The findings revealed that all of the isolates adhered.The mean optical density of all the isolates 0.226-0.723 ,The results are, classified into several groups, as illustrated in (Figs. 13 and 14). (A) Ten (34%) of the *P. aeruginosa* isolates produced biofilms with high adherence. (B) Fourteen (49%) isolates produced biofilms with moderate adherence. (C) Five (17%) isolates produced biofilms with poor adherence. According to the findings of this study, the existence of a strong or moderate biofilm allowed bacteria to cling strongly to any location in the host.Was selected 10 isolates of *P. aeruginosa* that were identical in their strength of biofilm production to conduct tests to study the inhibitory and antibacterial activity of CSNPs loaded BEO and BEO in addition to their effect on biofilm production.

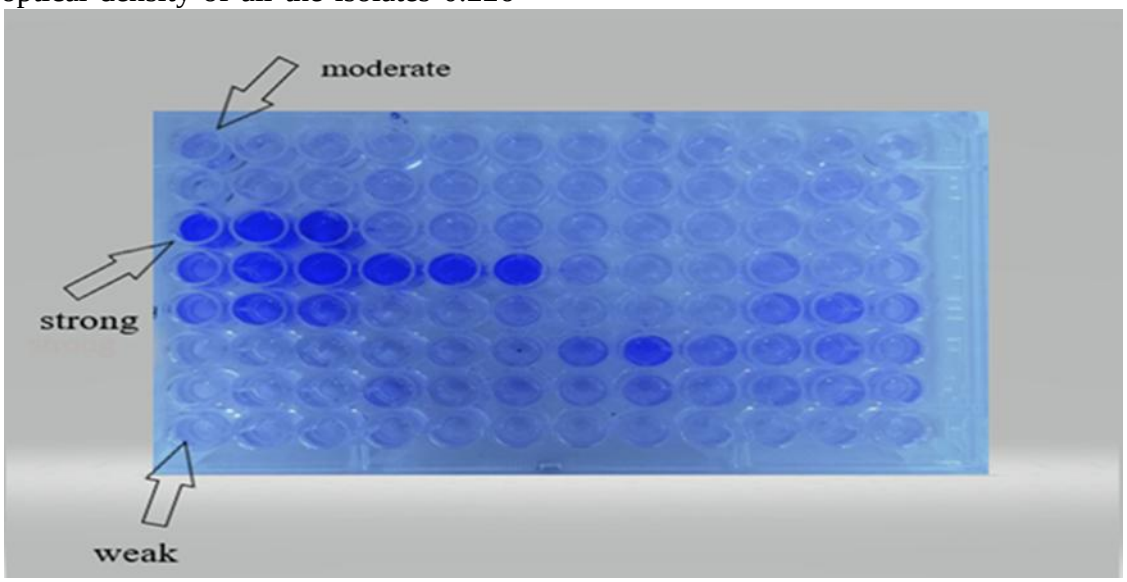

Figure 13. Quantitative assessment of biofilm development using a MTPl

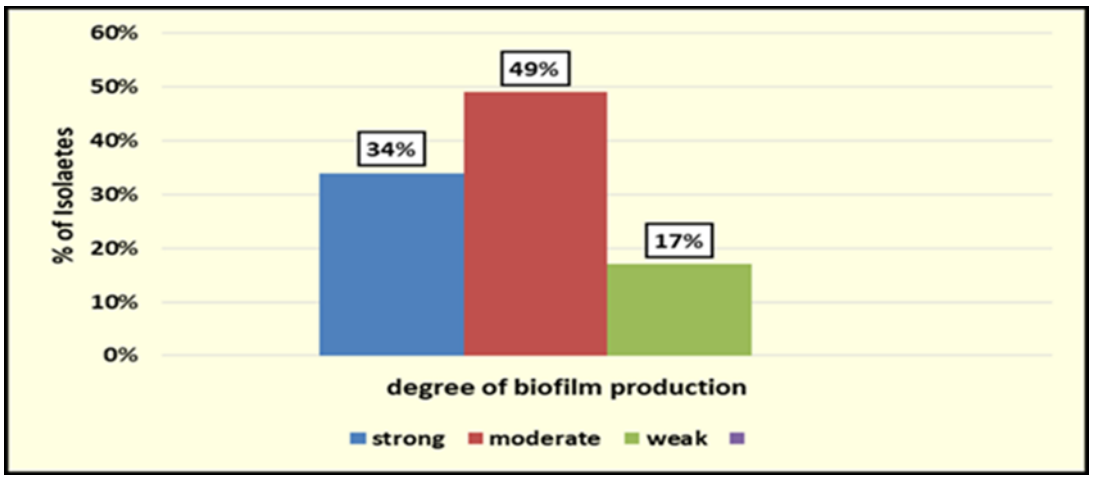

Figure 14. Percentage of biofilm production in *P.aeruginosa* isolates

Microtiter Plate Method (MTP) for Determining MIC: The minimum inhibitory concentration (MIC) of an antibacterial agent is defined as the lowest concentration that inhibits visible microbial growth after a specified incubation period. While clinical laboratories primarily use MIC values to determine bacterial resistance, they are also employed in research to assess the activity and establish MIC breakpoints of new antibacterial agents (5). The MIC values were calculated according to the concentration of active chemical constituents in BEO and BEO-loaded CSNPs, which are chiefly responsible for their therapeutic effects and account for 84.94% of *Ocimum basilicum L*. essential oil, as indicated by GC-MS analysis (Table 1). The concentration of these active compounds, estimated by HPLC (Table 4), was used to compare the minimum inhibitory concentrations of BEO and CSNPs loaded with BEO. The MIC against *P. aeruginosa* was measured using the microtiter plate technique in this investigation. Compared to the controls, the MIC and sub-MIC values were determined for the test substances against *P. aeruginosa* isolates. Initially, all wells appeared blue at the start of the assay; however, after 2–4 hours of incubation, some wells turned pink, indicating bacterial growth. As seen by the color change caused by bacterial growth, which decreases the resazurin dye from blue to resorufin with a pink hue in (Fig.15), When statistically interpreting and comparing the results of the MIC value between the BEO and the CSNPs loaded BEO, it was discovered that there is a difference in efficacy between the BEO and the CSNPs loaded BEO at ($P \leq 0.05$) .which indicates that the CSNPs-loaded BEO has greater antibacterial activity than the BEO alone. Significant differences were observed between the two groups. The MIC of BEO ranged from 190 to 95 µg/mL, whereas the MIC of BEO-loaded CSNPs was much lower, ranging from 3.75 to 0.93 µg/mL, representing the most effective concentrations for inhibiting *P. aeruginosa* growth. Sub-MIC values were also statistically analyzed, revealing a significant difference between BEO and BEO-loaded CSNPs at $P \leq 0.05$ (Table 5). Chitosan has been reported to exhibit antibacterial activity in vitro in several studies. The antibacterial effect of CSNPs is primarily attributed to their interactions with the bacterial cell wall or cell membrane, and multiple mechanisms have been proposed to explain this activity (13). The most widely described mechanism involves electrostatic interactions between the positively charged amino groups of glucosamine and the negatively charged bacterial membranes. This interaction causes extensive alterations to the cell surface, leading to changes in membrane permeability, osmotic imbalance, and leakage of intracellular contents, ultimately resulting in bacterial cell death (30). The significance of nanotechnology in drug delivery lies in its ability to enhance the therapeutic efficacy of drugs by increasing the surface area through reduced particle size, allowing drugs to reach target sites more efficiently at lower doses. This approach not only minimizes potential side effects associated with chemical drugs but also provides an economically advantageous strategy (22).

Table 5. The MIC and Sub-MIC value of CSNPs loaded BEO and BEO on *P. aeruginosa* by Resazurin aided microdilution method

Isolates	CSNPs / BEO MIC	BEO MIC	LSD	CSNPs/ BEO Sub-MIC	BEO Sub-MIC	LSD
P1	1.87	190	16.72 *	0.93	95	8.61 *
P11	3.75	190	16.04 *	1.87	95	8.07 *
P12	0.93	95	12.36 *	0.46	47.5	6.53 *
P14	3.75	95	13.42 *	1.87	47.5	6.59 *
P15	3.75	190	16.04 *	1.87	95	8.07 *
P16	3.75	95	13.42 *	1.87	47.5	6.59 *
P17	3.75	95	13.42 *	1.87	47.5	6.59 *
P18	1.87	190	16.72 *	0.93	95	9.61 *
P21	3.75	95	13.42 *	1.87	47.5	6.59 *
P22	3.75	95	13.42 *	1.87	47.5	6.59 *
LSD	2.07 *	18.64 *	---	1.37 *	13.72 *	---

* (P≤0.05).

***Significant**

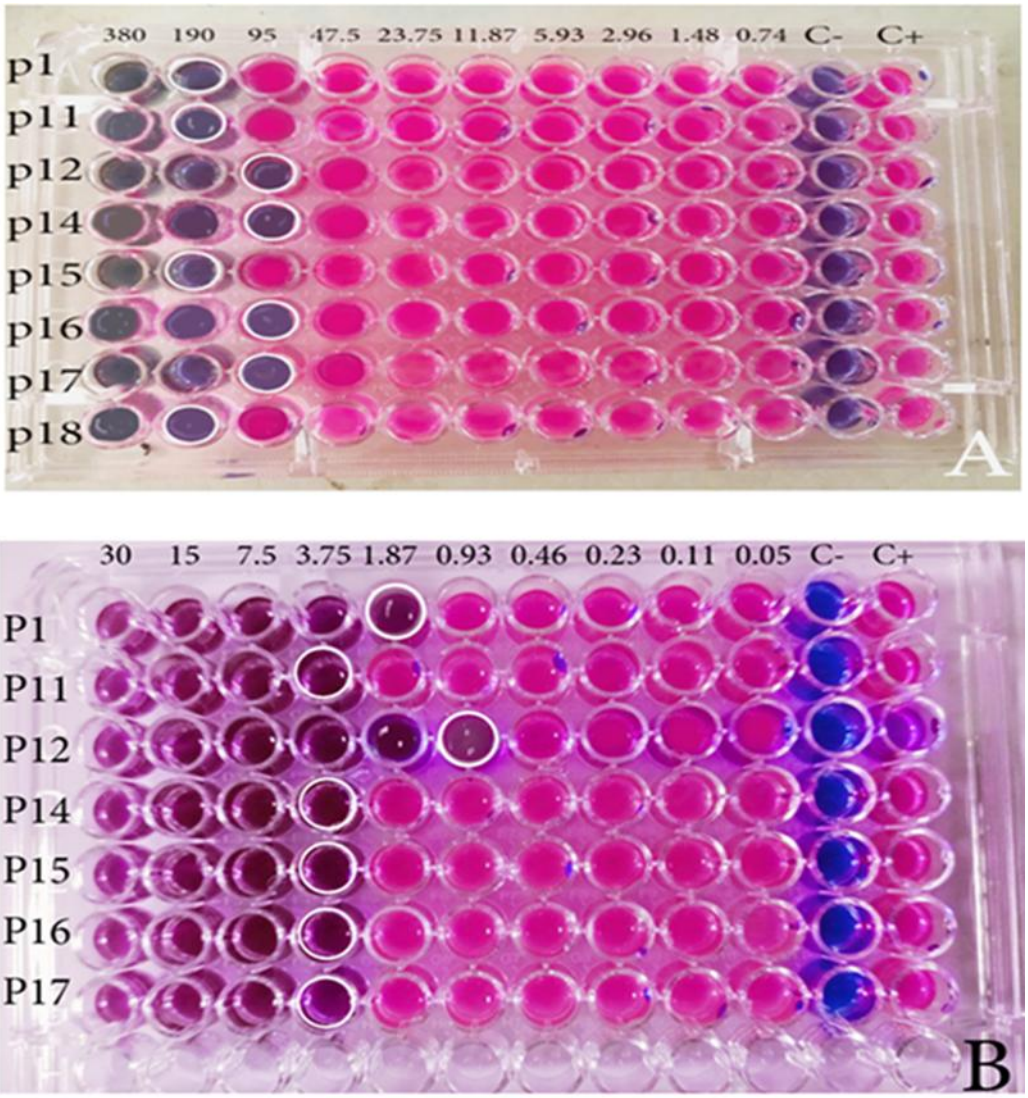

Figure 15. MTP 96-well of (A) (BEO)and (B)(CSNPs loaded BEO) on *P. aeruginosa* isolates

Substance Efficacy Detection Against Biofilm Production: Using the sub-minimal inhibitory concentrations (sub-MICs), the effect of the test compounds on the formation or inhibition of biofilms by strong biofilm-producing *P. aeruginosa* isolates was evaluated. The percentage of biofilm inhibition was determined using Equation (4), with the results presented in (Table 6). The data indicate a notable reduction in optical density following treatment with the test compounds. The biofilm inhibition activity of CSNPs loaded BEO is stronger in isolates P16 and P22, with 84.28% and 79.32%, respectively. In comparison to BEO inhibitory activity, the isolates P16 and P22 had also greater inhibition percentages of 66.74% and 57.43%, respectively. The lower inhibition activity for CSNPs loaded BEO was 51.32% for P1, whereas the lower inhibition percent of BEO was 39.43% in isolate P21. The results demonstrated significant differences ($P \leq 0.05$) between the majority of treatments (BEO and CSNPs loaded with BEO). with CSNPs loaded BEO being considerably better than BEO in terms of increasing the percentage of *P. aeruginosa* biofilm production that was inhibited. Plant extracts incorporated into nanoparticles play dual roles, serving as both reducing and stabilizing agents. Phenolic and flavonoid compounds act as reducing agents, whereas amino acids function as stabilizers. Together, these properties contribute to an enhanced activity of the nanoparticles. (8). The activity of nanoparticles is enhanced due to these characteristics. Exposure of multidrug-resistant *P. aeruginosa* to essential oils effectively loaded into chitosan nanoparticles results in a significant increase in antibacterial activity. The current results support those of (16), who observed that chitosan nanoparticles generated by the ionic gelation process have potent antibacterial properties against Gram-negative bacteria. The electrostatic force that exists between the CSNPs-loaded BEO and the bacterial cell wall, promoting a stronger bond with charged molecules, allows the BEO to pass through the cell wall.Three mechanisms have been proposed to explain chitosan's ability to interact with the cell wall or outer membrane of Gram-negative bacteria and modulate their antibacterial activity:(a) The positively charged chitosan molecules bind electrostatically to the negatively charged residues on bacterial surfaces, altering cell membrane permeability. (b) Chitosan can penetrate bacterial cells and interact with DNA, inhibiting RNA transcription, mRNA synthesis, and protein production. (c) Chitosan can chelate essential nutrients and minerals, thereby suppressing microbial growth (7).

Table 6. Biofilm inhibition percent of *P. aeruginosa* isolates after being treated with Sub-MIC of CSNPs loaded BEO and BEO

Isolates	%Control Biofilm	% Inhibition CSNPs loaded BEO	% Inhibition BEO	LSD
P1	100	51.32	47.84	12.77 *
P11	100	65.26	49.65	11.94 *
P12	100	54.76	41.43	11.25 *
P14	100	76.42	47.98	14.68 *
P15	100	59.22	52.71	11.94 *
P16	100	84.28	66.73	14.62 *
P17	100	74.32	53.65	14.05 *
P18	100	56.83	52.87	12.91 *
P21	100	51.76	39.43	14.37 *
P22	100	79.32	57.43	15.02 *
LSD	NS	12.83 *	14.05 *	---

* (P≤0.05).

***Significant**

CONCLUSIONS

According to the resulrs, the following conclusions may be . The current findings indicate that basil contains bioactive secondary metabolites (phytochemicals) capable of inhibiting microbial growth. The vital activity of essential oil extracted from basil leaves increases against some pathogenic bacteria The largest percentage of the essential oil of basil is Linalool. *Pseudomonas aeruginosa* isolates produced biofilm at three distinct levels of intensity: strong, moderate, and weak. A novel green strategy was established

for the synthesis of antimicrobial nanoparticles by chemically cross-linking two biomolecules to create a stable structure. In this approach, chitosan nanoparticles loaded with *Ocimum basilicum* essential oil (BEO) were synthesized biologically, using TPP as a cross-linking agent. The findings of the present study confirmed that the BEO-loaded chitosan nanoparticles were chemically stable, exhibited a spherical morphology with high crystallinity, and had particle sizes ranging from 50.31 to 64.09 nm. The sub-MIC concentrations of BEO-CSNPs demonstrated a significant inhibitory effect on biofilm formation by *Pseudomonas aeruginosa*, with effective concentrations ranging from 0.93 to 3.75 µg/ml. In conclusion, BEO-loaded chitosan nanoparticles effectively inhibited biofilm production by *Pseudomonas aeruginosa* isolates obtained from burn infections.

CONFLICT OF INTEREST

The authors declare that they have no conflicts of interest.

DECLARATION OF FUND

The authors declare that they have not received a fund.

REFERENCES

1. Allahverdiyev, A. M.; V. Kon, K..; Abamor, E. S.; M. Bagirova, and M. Rafailovich. Coping with antibiotic resistance: combining nanoparticles with antibiotics and other antimicrobial agents. Expert review of anti-infective therapy. (2011). 9(11): 1035-1052. https://doi.org/10.1586/eri.11.121

2. Almatroudi, A. 2024. Investigating Biofilms: Advanced Methods for Comprehending Microbial Behavior and Antibiotic Resistance. *Frontiers in Bioscience*, 29(4), 133. https://doi.org/10.31083/j.fbl2904133

3. Amelia, B.; E. Saepudin,; A. H. Cahyana.; D.U.Rahayu.; A. S. Sulistyoningrum,. and J. Haib,2017 GC-MS analysis of clove (Syzygium aromaticum) bud essential oil from Java and Manado. AIP Conference Proceedings, 1862: 030082-1–82-9. https://doi.org/10.1063/1.4991186

4. Aydin, R. and M. Pulat,2012. 5-Fluorouracil encapsulated chitosan nanoparticles for pH-stimulated drug delivery: evaluation of controlled release kinetics. J. Nanomater. . 42:56-58. https://doi.org/10.1155/2012/313961

5. Ayesha, J., and A. Despeina, 2024. Antibiotic susceptibility testing using minimum inhibitory concentration (MIC) assays. Nature Reviews Microbiology, 22(4), 215–228. https://doi.org/10.1038/s44259-024-00051-6

6. Chandra Dey, S.; Al-Amin, M.; Ur Rashid, T.; Zakir Sultan, M.; Ashaduzzaman, M.; Sarker and et al. 2016. Preparation, characterization, and performance evaluation of chitosan as an adsorbent for remazol red. International Journal of Latest Research in Engineering and Technology,2(2): 52–62.

7. Chen, C. Z. and S. L. Cooper. 2002. Interactions between dendrimer biocides and bacterial membranes. Biomaterials 23(16), 3359–3368. https://doi.org/10.1016/S0142-9612(02)00036-4

8. Chenthamara, D.; S. Subramaniam, S. G. Ramakrishnan,; S.Krishnaswamy; M. Essa; F.H. Lin, and et al.2019. Therapeutic efficacy of nanoparticles and routes of administration. Biomaterials Research, 23(1):1–29. DOI:10.1186/s40824-019-0166-x

9.Elshikh, M.; S. Ahmed,; S. Funston; P. Dunlop,; M. McGaw; R. Marchant, et al. 2018. Resazurin-based 96-well plate microdilution method for the determination of the minimum inhibitory concentration of biosurfactants. Biotechnology Letters, 38(6):1015–1019. https://doi.org/10.1007/s10529-016-2079-2

10. Emad M, Bader Y, Ralciane de. Back to nature: Medicinal plants as promising sources for antibacterial drugs in the post-antibiotic era. Plants. 2023;12(17):3077. https://doi.org/10.3390/plants12173077

11. Gowda, M., and S. Ramachandra, 2024. A validated comparative study of RP-HPLC, GCFID, and UV spectrophotometric methods for the quantification of eugenol isolated from Syzygium Aromaticum L. Journal of Pharmacognosy and Phytochemistry 2024; 13(5): 544-550 DOI: 10.22271/phyto 2024.v13.i5h.15123

12. Haney, E. F.; M. J. Trimble, and R. E. Hancock. 2021. WMicrotiter plate assays to assess antibiofilm activity against bacteria. Nature Protocols, 16(5):2615–2632.

DOI:10.1038/s41596-021-00515-3.
https://doi.org/10.1038/s41596-021-00515-3
13. Helander I M, E. L Nurmiaho-Lassila, R. Ahvenainen, J. Rhoades, S. Roller. 2001. Chitosan disrupts the barrier properties of the outer membrane of Gram-negative bacteria. International Journal of Food Microbiology.71:235244.
https://doi.org/10.1016/S0168-1605(01)00609-2
14. Hemmati, J., and M. Nazari, 2024. *In vitro* investigation of relationship between quorum-sensing system genes, biofilm forming ability, and drug resistance in clinical isolates of *Pseudomonas aeruginosa.* BMC Microbiology, 24, Article 99.
https://doi.org/10.1186/s12866-024-03249-w
15. Jahed, E., M. A. Khaledabad, M. R. Bari, and M, H. Almasi. 2017. Effect of cellulose and lignocellulose nanofibers on the properties of Origanum vulgare ssp. gracile essential oil-loaded chitosan films. React. Funct. Polym. 117,70–80.
https://doi.org/10.1016/j.reactfunctpolym.2017.06.008
16. Javed, R.; M. Zia, ;S. Naz, ; S.O. Aisida, and Q. Ao, 2020. Role of capping agents in the application of nanoparticles in biomedicine and environmental remediation: recent trends and prospects. Journal of Nanobiotechnology, 18(1): 1–15.
https://doi.org/10.1186/s12951-020-00704-4
17. Jawad, A. Mohammed, K. Asmahan Allawi1, Hind Mufeed Ewadh.2018 Essential oils of rosemary as antimicrobial agent against three types of bacteria. Med J Babylon ;15:53-6. DOI:10.4103/MJBL.MJBL_14_18
18. Jha A. K, K. Prasad, and A. Kulkarni. 2009. Plant system: nature's manufactory. Coll Sur B: Biointerfaces.73: 219-223. DOI:10.1016/j.colsurfb.2009.05.018
19. kadhum, W. N. and I. A. Al-Ogadi, 2022 Evaluation of chitosan-alginate nanoparticle as A stable antibacterial formula in biological fluids.iraqi Journal of Science,Vol. 63, No. 6, pp:23982418.
https://doi.org/10.24996/ijs.2022.63.6.8
20. Khan, I.; K. Saeed, and I. Khan, 2015. Nanoparticles: Properties, applications, and toxicities. Arabian Journal of Chemistry, 12(7): 908–931.
https://doi.org/10.1016/j.arabjc.2017.05.011
21. Kim, J. A., Y. J. Cho, and H. S. Lim, 2022. Assessment of the biofilm-forming ability on solid surfaces of periprosthetic infection-associated pathogens. Scientific Reports, 12, Article 22929.
https://doi.org/10.1038/s41598-022-22929-z
22. Kowalska-Krochmal, B. and R. Dudek-Wicher. 2021. The minimum inhibitory concentration of antibiotics: methods, interpretation, clinical relevance. Pathogens, 10(2):165.
https://doi.org/10.3390/pathogens10020165
23. Mahmood, H., Nasir, G., and Q. Ibraheem, 2020. Relationship between pigment production and biofilm formation from local Pseudomonas aeruginosa isolates. Iraqi Journal of Agricultural Science, 51(5), 1413-1419.
https://doi.org/10.36103/ijas.v51i5.1151
24. Menakera, M. Kravetsb, M. Koela, and A. Orava, 2004. Identification and characterization of supercritical fluid extracts from herbs, C. R. Chimie7629–633. DOI:10.1016/j.crci.2004.03.005
25. Muller, R. H., C. Jacobs, and O. Kayser, 2001. Nanosuspensions as particulate drug formulations: rationale for development and what we can expect for the future. Adv. Drug Deliv. Rev. 47, 3–19.
https://doi.org/10.1016/S0169-409X(00)00118-6
26. Mustafa H. N. I. Al –Ogaid. 2023. Efficacy of zinc sulfide–chitosan nanoparticles against bacterial diabetic wound infection. Iraqi Journal of Agricultural Sciences ,54(1):1- 17
https://doi.org/10.36103/ijas.v54i1.1671
27. Nasti, A.; N. M. Zaki, ; P. De Leonardis.; S. Ungphaiboon,; P. Sansongsak,; M. J. Rimoli, et al. 2009. Chitosan/TPP and chitosan/TPP-hyaluronic acid nanoparticles: Systematic optimization of the preparative process and preliminary biological evaluation. Pharmaceutical Research, 26(8):1918–1930.
https://doi.org/10.1007/s11095-009-9908-0
28. Nirwati, H., K. Sinanjung, , F. Fahrunissa, F. Wijaya, S. Napitupulu, V. P. Hati, T. Nuryastuti, 2019. Biofilm formation and antibiotic resistance of *Klebsiella pneumoniae* isolated from clinical samples in a tertiary care hospital, Klaten, Indonesia. BMC Proceedings,

13(11), 1–8. https://doi.org/10.1186/s12919-019-0176-7

29. Olajire, A. A. and A. A. Mohammed. 2020. Green synthesis of bimetallic Pd core Au shell nanoparticles for enhanced solid-phase photodegradation of low-density polyethylene film. J. Mol. Struct.1206, 127724. https://doi.org/10.1016/j.molstruc.2020.127724

30. Raafat D., K.von Bargen, A.Haas., and H. Sahl. 2008. Insight into the mode of action of Chitosan as an Antibacterial Compound. Applied and Environmental Microbiology. 74: 3764-3773.Research; 7(5); 251-257. https://doi.org/10.1128/AEM.00453-08

31. SAS. 2018. Statistical Analysis System, User's Guide. Statistical. Version 9.6th ed. SAS. Inst. Inc. Cary. N.C. The US